

Midfrontal theta is associated with errors, but no evidence for a link with error-related memory

Xiaochen Y. Zheng^{1*}, Syanah C. Wynn^{1,2*}

¹ Donders Institute for Brain, Cognition and Behaviour, Radboud University, Nijmegen, The Netherlands

² Centre for Human Brain Health, School of Psychology, University of Birmingham, Birmingham, UK

** XYZ and SCW contributed equally to the work.*

Correspondence to:

Syanah C. Wynn

Centre for Human Brain Health

School of Psychology

University of Birmingham

Birmingham B15 2TT, UK.

E-mail: s.wynn@bham.ac.uk.

Abstract

Midfrontal theta is widely observed in situations with increased demand for cognitive control, such as monitoring response errors. It also plays an important role in the cognitive control involved in memory, supporting processes like the binding of single items into a memory representation or encoding contextual information. In the current study, we explored the link between midfrontal theta and error-related memory. To this end, we recorded EEG from 31 participants while they performed a modified flanker task. Their memory for the errors made during the task was assessed after each experimental block, and its relationship with error-related midfrontal theta effects was investigated. We have replicated the error-related increase in midfrontal theta power, reported in previous literature. However, this error-related theta effect could not predict subsequent memory of the committed errors. Our findings add to a growing literature on the prefrontal cortex-guided control process in error monitoring and memory.

Keywords: theta oscillations, recollection, error monitoring, prefrontal cortex

Introduction

When we make a mistake, our brain sets in motion processes to prevent us from making additional mistakes. To learn from our errors, we need to monitor them and adjust our behavior accordingly. This happens on different timescales, in the milliseconds following an error, the brain needs to identify the event as an error to adjust immediate behavior accordingly. For instance, when accidentally hitting the gas pedal instead of the brake, our brain needs to quickly send a signal to our feet to initiate a motor response to correct this. In addition, we need to be able to remember the errors we made in the past to prevent them from happening again. The next time you step in a car you will remember the error you made hours, days, or weeks ago and you will be mindful of not making the same mistake again. Therefore, our brain needs the joint efforts of error-related and memory-related processes for us to learn from our mistakes in daily life.

The detection of an error is reflected by midfrontal theta oscillations (4-7 Hz), recorded from electroencephalography (EEG) channels over the medial prefrontal cortex (PFC; Cavanagh & Frank, 2014; Cohen, 2011a; Fusco et al., 2018; Kalfaoğlu, Stafford, & Milne, 2018). Neural oscillations are thought to be important for transient brain computations needed for cognitive functions, and theta appears to coordinate processes needed for post-error cognitive control (Bonnetfond, Kastner, & Jensen, 2017; Duprez, Gulbinaite, & Cohen, 2020; Fries, 2005; Jensen, Gips, Bergmann, & Bonnetfond, 2014; Kalfaoğlu et al., 2018). During various tasks, midfrontal theta power is increased around -100 to 500ms relative to error commission (Kalfaoğlu et al., 2018; Novikov, Bryzgalov, & Chernyshev, 2015; Trujillo & Allen, 2007; Yordanova, Falkenstein, Hohnsbein, & Kolev, 2004). Moreover, when participants are given the opportunity to correct committed errors, midfrontal theta can predict subsequent error corrections (Kalfaoğlu

et al., 2018). This suggests that midfrontal theta reflects processes involved in error awareness and the subsequent post-error cognitive control. In addition, when applied externally through transcranial alternating current stimulation (tACS), midfrontal theta modulated behavioral adjustments following errors in a flanker task (Fusco et al., 2018). It is thought that midfrontal theta originates from the anterior cingulate cortex (ACC) and is cognitively associated with the monitoring of the errors (Botvinick, Cohen, & Carter, 2004; Cavanagh, Cohen, & Allen, 2009; Chevalier, Hadley, & Balthrop, 2021; Cohen, 2011a). The increase in midfrontal theta may signal an increased need for top-down control to adjust behavior, recruiting the PFC to prevent subsequent errors (Cavanagh, Zambrano-Vazquez, & Allen, 2012; Cohen, 2011a; Kerns, 2006). Given this involvement of midfrontal theta in real-time error adjustments, it would be of interest to know if theta encodes error-related information that can predict error memory at a later point in time. If this is the case, it suggests that midfrontal theta can influence behavioral adjustments on a timescale of minutes or even longer.

We know that theta oscillations play a role in various stages of memory processes, including the encoding of new information. Intracranial and scalp EEG studies have shown that encoding-related theta power is greater for items that are later remembered, as compared to those that are later forgotten (Simon Hanslmayr, Spitzer, & Bäuml, 2009; Nyhus & Curran, 2010b; Osipova et al., 2006; Sederberg, Kahana, Howard, Donner, & Madsen, 2003; Sederberg et al., 2007; White et al., 2013; Wynn, Daselaar, Kessels, & Schutter, 2019). These effects are the most pronounced 300-1000ms after stimulus onset over frontocentral regions. Additionally, Cohen (2011b) utilized a combined EEG-MRI design to show a close interplay between hippocampal-PFC connectivity, midfrontal theta and long-term memory performance. This is in line with other studies proposing that memory-related theta mediates PFC-guided control processes needed for

task-relevant encoding (Cavanagh & Frank, 2014; Nyhus & Badre, 2015; Nyhus & Curran, 2010a). This supports the idea that midfrontal theta mediates processes that are needed for memory, like the binding of single items into a memory representation or encoding contextual information (Hsieh & Ranganath, 2014). Therefore, midfrontal theta appears to play a supporting role in both error monitoring and memory encoding.

In the current study, we aimed to bridge the error- and memory-related literature by exploring the link between midfrontal theta and error-related memory. If midfrontal theta during error commission can predict subsequent error memory, this would suggest that midfrontal theta plays an important role in the encoding of errors into memory. This could provide an initial indication that midfrontal theta is not only involved in momentary error awareness right after an erroneous response, but also in learning from errors on a longer time scale (e.g., to prevent new errors in the future). Our participants performed a modified flanker task (Eriksen & Eriksen, 1974), while we assessed their error memory after each experimental block. This enabled us to explore if midfrontal theta reflects the online detection of the errors and will predict participants' memory of the errors they have made. We predict that midfrontal theta is involved in both error detection and the encoding of the error. Therefore, we hypothesized that (1) we would replicate the increase in midfrontal theta after error commission, and (2) this error-related theta effect would be a significant predictor of the ability to recall the number of errors made.

Methods

Participants

A total of 31 healthy right-handed adults participated in this study, recruited through the Radboud Research Participation System. All had normal or corrected-to-normal vision, were

native Dutch speakers, and were free from any self-reported neurological or psychiatric conditions. All participants received course credit or monetary compensation. Of these 31 participants, four participants were excluded from the analyses reported here, due to limited number of trials left after artifact rejection (N=1), chance-level performance during the flanker task (N=1), or data acquisition issues (N=2) that rendered the data unusable for data analyses reported here. This results in a total 27 participants (15 females, 12 male, $M_{\text{age}} = 22.52$, $SD_{\text{age}} = 3.91$) reported in the current analyses. One additional participant without working memory (WM) measures was excluded from the correspondent analysis. The study was approved by the local ethics committee of the Faculty of Social Sciences of the Radboud University Nijmegen.

Procedure

All participants received written information prior to participation but remained naive regarding the aim of the study. Upon arrival at the laboratory, all participants were screened for eligibility to participate in EEG studies and provided written informed consent.

Working memory task

Prior to the flanker task, a computerized version of the digit span task from the Wechsler Adult Intelligence Scale fourth edition (WAIS-IV; Kreutzer, DeLuca, & Caplan, 2011) was used as a measurement of WM. The digit span task consisted of three conditions (forward, backward, and sequencing) and the order of these was kept consistent across participants. During all conditions, a single digit (1-9) was presented centrally on the screen for 1000 ms, followed by a 300 ms inter-stimulus interval. Digit presentation and recording of responses were attained using PsychoPy (v1.80; Peirce et al., 2019) on a Windows PC. For each condition, every trial consisted of two series of digits, which increased by one digit on every trial (e.g., first trial: 3-5 and 8-4;

second trial: 9-5-2 and 1-7-6). In the forward condition, participants were asked to reproduce the digits in the same order as previously presented after each series (e.g., first trial: 3-5 and 8-4; second trial: 9-5-2 and 1-7-6). In the backward condition, they were asked to reproduce the series in the reversed order (e.g., first trial: 5-3 and 4-8; second trial: 2-5-9 and 6-7-1). In the sequencing condition, participants had to recall the digits in ascending order (e.g., first trial: 3-5 and 4-8; second trial: 2-5-9 and 1-6-7). Participants responded by typing the digit sequence on a keyboard. Participants were able to alter their response up to the moment of confirmation, which was operationalized by pressing the enter key. The task was aborted when a participant was not able to respond correctly in both two series in a single trial. The total number of correct responses was used as their WM score. The maximal score that could possibly be obtained was 16 for all three conditions.

Flanker task

Thereafter, participants performed a modified flanker task (Eriksen & Eriksen, 1974), where they were required to give a speeded response to a central target arrow, while ignoring congruent (“>>>>” or “<<<<”) or incongruent (“>><<” or “<<>>”) flanker arrows (see Figure 1). Half of the trials were congruent, and half were incongruent. Participants responded to the target arrows by pressing the “D” key (left arrows) and the “H” key (right arrows) on a keyboard, with their left and right index fingers, respectively. Stimuli were presented on a grey background for 200 ms, with stimulus onset asynchronies randomly selected from a uniform distribution with a mean of 1550 ms and varying between 1400 and 1700 ms with 50 ms increments. During the intertrial interval, a white cross was centrally presented, and participants were instructed to keep fixation on the cross.

To elicit enough errors, we trained the participants to respond within a time limit prior to the main task. The time limit (*range* 336 - 640 ms, *mean* = 438 ms, *SD* = 74 ms) was computed dynamically across the training and calibrated individually for each participant (based on the 70 percentile of previous ten trials). If participants failed to respond within a given time limit, the fixation cross became red as a warning. The speed training consisted of 100 trials.

The main task that followed, was divided into six blocks of 100 trials. Participants were not given feedback on their performance during the main task, they were also allowed to respond after exceeding the time limit for each trial (i.e., slow trials). At the end of each block, participants were instructed to recall their task performance. Specifically, after each block, participants were asked to recall the number of errors made in the preceding block and rate their confidence in this judgment. To minimize any influence on task strategy, we also asked them to recall the number of times they felt their response was too slow in the preceding block. The numerical responses were given with the numbers on the keyboard, and the confidence ratings were submitted by clicking with a mouse on a visual analog scale, ranging from “completely not sure” to “completely sure”. The scale ranged from 0-100, although these values were not presented to the participants.

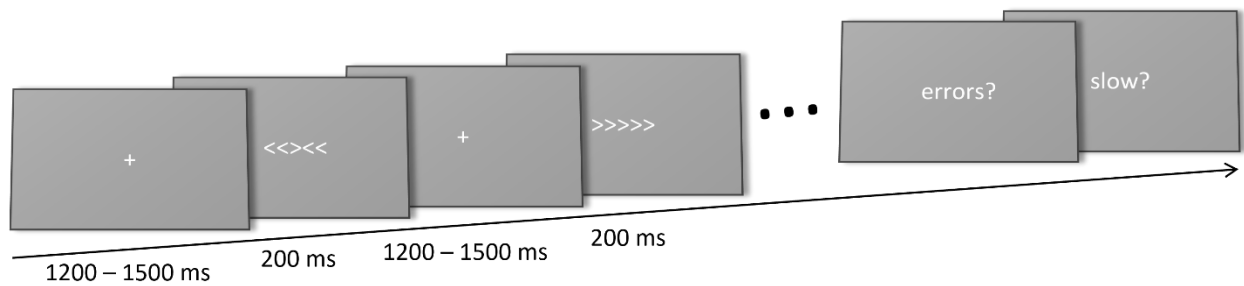


Figure 1. A schematic representation of the experimental task. After each flanker block, participants were asked to recall the number of errors made and the number of times they responded too slow in the preceding flanker block.

EEG acquisition

EEG signals were recorded during the flanker task (see Figure 1) and amplified with a BioSemi ActiveTwo system (BioSemi B.V., Amsterdam) from 32 Ag/AgCl-tipped electrodes, conforming to the International 10-20 System. The EEG signal was digitized at a sampling rate of 1024 Hz. Reference electrodes were placed bilateral on the mastoids, and bipolar electro-oculogram recordings were obtained from electrodes placed 1 cm lateral of the outer canthi, and above and below the left eye. Each active electrode was measured online with respect to a Common Mode Sense (CMS) active electrode. BioSemi uses a combination of a CMS electrode and a Driven Right Leg (DRL) passive electrode to ensure that the CMS electrode stays as close as possible to the reference voltage at the analogue-to-digital converter.

Data Analysis

Data analyses were performed in MATLAB (v2021a; MathWorks Inc., Natick MA) in combination with Fieldtrip toolbox (v20200128; Oostenveld, Fries, Maris, & Schoffelen, 2011), and in R (Version 4.0.2; R Core Team, 2013).

EEG pre-processing

Continuous data were first re-referenced to linked-mastoid references and then band-pass filtered with a low cut-off of 0.1 Hz and a high cut-off of 30 Hz. We then segmented the data into epochs from 500 ms before to 1400 ms after stimulus onset. Trials with atypical artifacts (e.g., jumps and drifts) as well as bad channels (less than 0.3%) were rejected by visual inspection; EOG artifacts (eye blinks and saccades) were removed using independent component analysis. After ICA, we reconstruct the earlier rejected channels by a weighted average of the data from neighboring channels of the same participant. The data were further segmented into epochs from 500 ms before to 800 ms after response onset. In an additional round of visual inspection, trials with remaining artifacts were removed.

Time-frequency analysis

To determine the time window that was sensitive to error-related processes, a cluster-based permutation on the time-frequency representations (TFRs) was performed (Maris, 2012; Maris & Oostenveld, 2007). First, spectral power was extracted using Fourier analysis with 500ms sliding time windows and the application of a Hanning taper. Data was symmetrically zero padded to two seconds and frequencies were assessed from 1 to 30 Hz in 1 Hz steps. Then TFRs of all error and correct trials were pooled together across participants. Based on the midfrontal theta literature (e.g., Cavanagh & Frank, 2014; Cohen, 2011a; Fusco et al., 2018), we restrict all our analysis to a selection of frontal midline channels (FC1, FC2, Fz, Cz) and the theta frequency band (4 - 7 Hz). We averaged the data in the channels and frequencies of interest in this analysis. To explore the effect in the time domain, all time points (i.e., -500 to 800 ms, time locked to the response onset) were included in the analysis. For every sample, the error and correct conditions were compared by means of a *t*-value. All samples with an α -value smaller than .05 were

selected and clustered. The corresponding cluster-level statistics were calculated by taking the sum of the t -values within each cluster. The largest cluster-level statistic was used as the observed cluster-based test statistic. The cluster-based test statistic distribution was approximated utilizing the Monte Carlo method with 10,000 random partitions. The proportion of random partitions that resulted in a larger test statistic than the observed one (the Monte Carlo significance probability) was compared to the critical α -value of .05 (two-sided). If the Monte Carlo significance probability was smaller than .05, the data in the error and correct conditions were considered significantly different.

Trial-by-trial frequency analysis

To be able to look at theta power over trials, the data was first re-segmented to the 0-500 ms time window, relative to response onset and then symmetrically zero padded to 1 second. This time window was chosen based on the results of the TFR analysis. For every trial, Fourier analysis was used to obtain the spectral decomposition of this data, using a Hanning taper. This gave the average theta power over the frontocentral channels in the 0-500 ms time window after response onset for each trial.

Mixed-effect models

The error memory performance per block was calculated as:

$$\frac{|Error_{recall} - Error_{true}|}{Error_{true}}$$

Where $Error_{recall}$ is the number of errors the participants remembered and $Error_{true}$ the actual number of errors made.

For the error-related midfrontal theta effect, we used the data from the trial-by-trial frequency analysis. Per participant and per block, the average theta power difference between error and correct trials was calculated as:

$$\frac{Theta_{error} - Theta_{correct}}{mean(Theta_{correct}, Theta_{error})}$$

We used linear mixed-effects models utilizing the lme4 package (Version 1.1.27; Bates et al., 2011). Errors and RTs were modeled trial by trial. The errors were analyzed using generalized linear mixed-effects models (binomial family), as a function of flanker congruency, post-error status (i.e., whether the current trial followed an error trial), WM score, and block number. Flanker congruency and post-error status were included as random slopes for participants. RT data were log-transferred to account for its right-skewed distribution. We additionally included accuracy as a fixed effect as well as a random slope for participants when modeling the RTs.

```
lmer(log(RT) ~ congruency + accuracy + post_error + WM_sum + ordered(Block) + (1 + congruency + accuracy + post_error | participant), data = data_by_trial, control = lmerControl(optimizer = "bobyqa"))
```

```
glmer(accuracy ~ congruency + post_error + WM_sum + ordered(block) + (1 + congruency + post_error | participant), data = data_by_trial, family = "binomial", control = glmerControl(optimizer = "bobyqa"))
```

Error memory performance was modeled by block. To account for the left-skewed distribution of the error memory scores, we used a generalized linear mixed model with a zero-inflated gamma distribution (glmmTMB package, Brooks et al., 2017). We modeled error memory as a function of the error-related midfrontal theta effect, error rate, WM score, and block number. Error rates were included as a random slope for participants.

```
glmmTMB(error_memory_abs ~ theta_effect + error_rate + WM_sum + ordered(block) + (1 + error_rate | participant), data = data_by_block., family = ziGamma(link = "log"), ziformula = ~1)
```

In addition, we modelled whether the error-related theta effect could predict the sign of the error memory scores (i.e., under- vs. overestimation) using a generalized mixed effect model. To exclude the potential confound that participants using counting strategy to enhance error memory performance (i.e., when they were very confident about their guesses), we also included an interaction model using the confidence score reported after each block. All models used in the analyses are provided in Supplementary Material A. We centered all the continuous predictors for all the models.

Results

Flanker task performance and working memory

Participants' performance on the flanker task is shown in Figure 2. In line with the literature, participants showed a congruency effect; they were slower ($\beta = 0.16$, $SE = 0.01$, $t = 10.91$, $p < .001$) and made more errors ($\beta = 2.48$, $SE = 0.18$, $z = 13.92$, $p < .001$) in the incongruent than the congruent condition. In addition, they were faster when making an erroneous response as compared to a correct one ($\beta = -0.20$, $SE = 0.02$, $t = -12.46$, $p < .001$). We observed post-error slowing ($\beta = 0.02$, $SE = 0.01$, $t = 2.89$, $p = .008$), but no post-error accuracy change ($\beta = 0.07$, $SE = 0.06$, $z = 1.08$, $p = .28$). Over time, participants got faster ($\beta = -0.02$, $SE = 0.003$, $t = -4.85$, $p < .001$), but their accuracy remained the same ($\beta = -0.04$, $SE = 0.06$, $z = -0.65$, $p = .51$).

Participants' working memory performance was quantified as the total number of correct responses on the digit span task. Participant had an average total WM score of 32 ($M = 31.85$, $SD = 5.50$) over the three subtasks ($M_{\text{forward}} = 9.93$, $SD_{\text{forward}} = 2.09$; $M_{\text{backward}} = 10.81$, $SD_{\text{backward}} = 2.40$; $M_{\text{sequencing}} = 11.11$, $SD_{\text{sequencing}} = 2.50$). Their WM score could not predict their performance

on the flanker task (RT: $\beta < 0.001$, $SE = 0.002$, $t = 0.36$, $p = .73$; accuracy: $\beta = 0.02$, $SE = 0.02$, $z = 0.73$, $p = .47$).

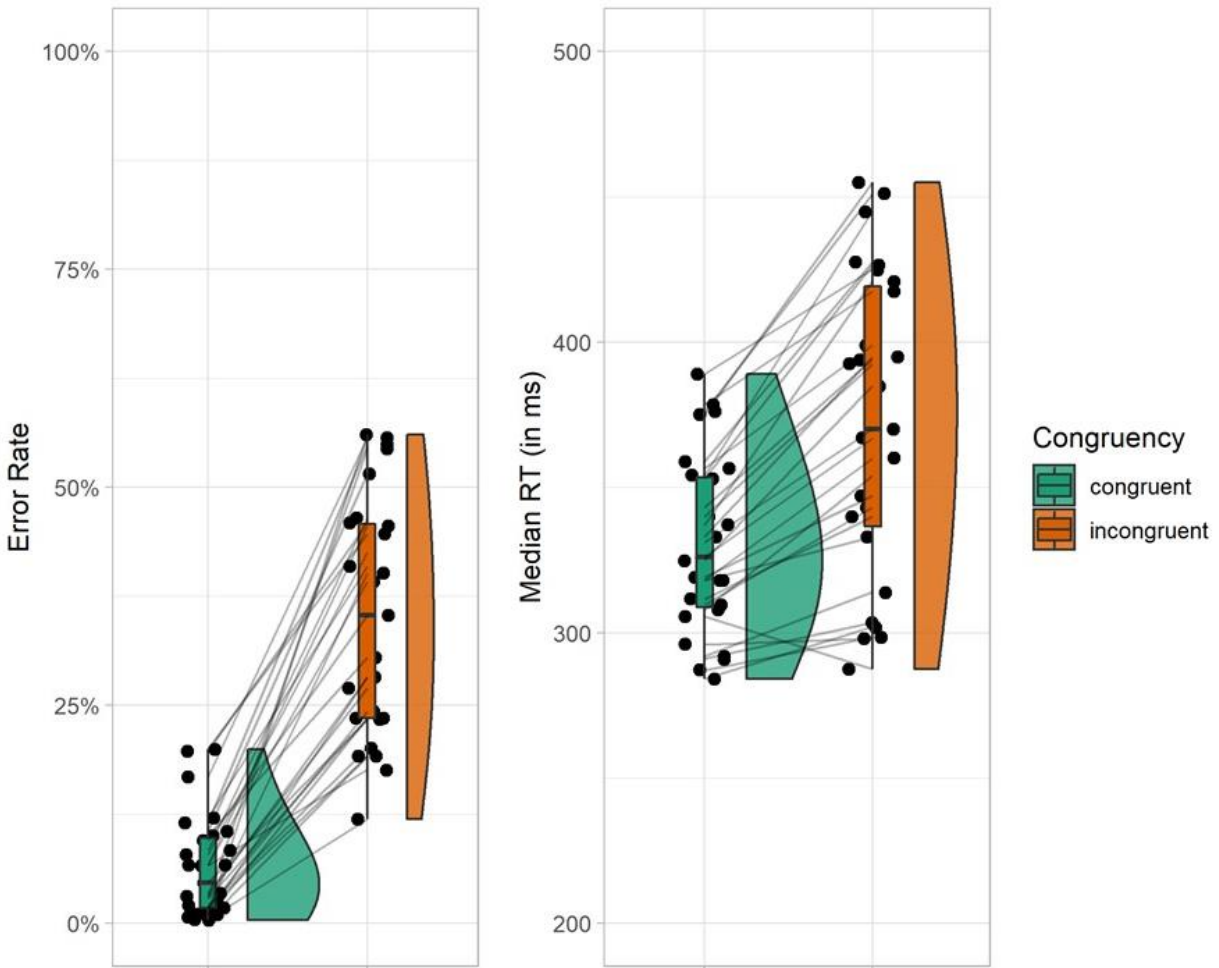


Figure 2. Raincloud plots of error rate (left panel) and median reaction time (RT, in ms, right panel) as a function of trial congruency. The outer shapes represent the distribution of the data over participants, the thick horizontal line inside the box indicates the group median, and the bottom and top of the box indicate the group-level first and third quartiles of each condition. Each dot represents one participant, the thin lines in between connect the same participant's data for different conditions.

Midfrontal theta is modulated by flanker errors

We explored whether theta power was modulated by flanker performance, as suggested by the literature (e.g., Nigbur, Ivanova, & Sturmer, 2011), and inspect the temporal nature of this effect. When we look at **Error! Reference source not found.**, comparing error and correct trials, there appears to be an increase in theta power over midfrontal channels in the first 250 ms after an error is made. This observation was tested by a cluster-based permutation analysis on the TFRs, which revealed a significant positive cluster ($p < .001$). This indicates that midfrontal theta power increased significantly following an erroneous, compared to a correct response. This effect was most pronounced between -31 ms and 545 ms relative to response onset, based on inspection of this cluster, further analyses in the manuscript were restricted to 0-500 ms.

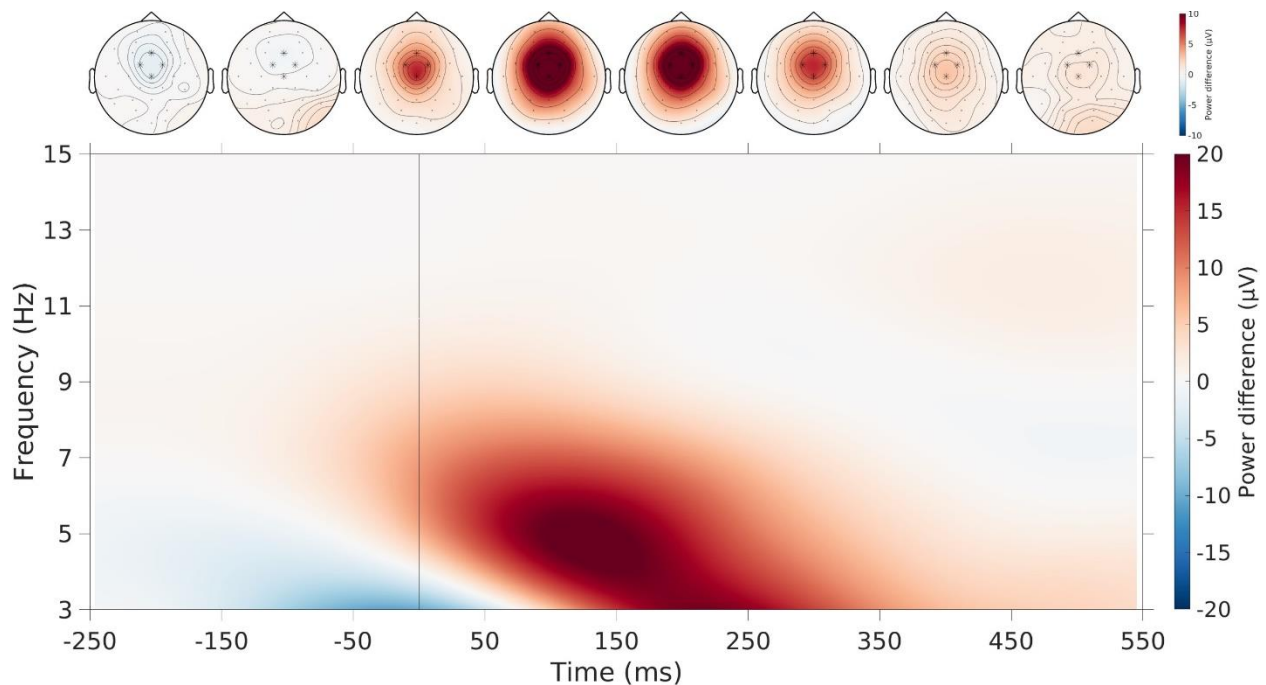


Figure 3. The theta power difference between error and correct trials over time. All time windows are relative to response onset. On the top row the topographical distribution of the

effect is plotted, with the midfrontal channels marked (FC1, FC2, Fz, Cz). The time-frequency representation for these midfrontal channels is plotted on the bottom row.

Error-related midfrontal theta cannot predict error memory performance

Participant' ability to remember their errors across blocks is visualized in Figure 4 (top panel). As can be seen in this figure, error memory performance increased over time ($\beta = 0.34$, $SE = 0.14$, $z = 2.35$, $p = .019$). Participants' confidence of their error memory (Figure 4, bottom panel) showed a wide range across participants and blocks, suggesting that they were unlikely to use strategies such as counting the errors.

Figure 5 (left panel) shows the relationship between participants' error-related theta effect during each flanker block and their error memory performance after each block. In general, it appears that there is no clear relationship between this neural theta effect and the memory performance. In addition, there also seems to be very little consistency between participants as can be seen in three example participants in the right panel of Figure 5. This observation was tested by utilizing a generalized linear mixed effects model. The model showed that error memory performance could not be predicted by the error-related midfrontal theta effect ($\beta = -0.03$, $SE = 0.22$, $z = -0.15$, $p = .88$). This indicated that contrary to our prediction, online modulation of error-related midfrontal theta was not predictive of later error memory. We also accounted for participants' WM score and their performance accuracy in the same model. Neither error rates ($\beta = -1.14$, $SE = 1.46$, $z = -0.78$, $p = .43$), nor participants' WM score ($\beta = -0.01$, $SE = 0.03$, $z = -0.46$, $p = .65$) affected their error memory performance. We further included the confidence measure to account for the situations where participants used a different strategy (e.g., counting, although unlikely). Neither does confidence predict error memory ($\beta = -$

0.004, $SE = 0.003$, $z = -1.24$, $p = .22$), nor does confidence interact with theta effect in predicting error memory ($\beta = -0.01$, $SE = 0.01$, $z = -1.35$, $p = .18$). To explore whether potentially any sub-components of the midfrontal theta (Beldzik et al., 2022; Zuure et al., 2020) could better predict the error memory performance, we ran additional post-hoc analyses on the phase-locked power, non-phase locked power (Cohen & Donner, 2013), and utilized a multivariate source separation approach (GED) to separate out midfrontal theta from additional theta sources (Cohen, 2022; Zuure, Hinkley, Tiesinga, Nagarajan, & Cohen, 2020). All these additional post-hoc analyses yielded comparable results to the ones reported above (i.e., midfrontal theta effect cannot predict error memory). Details on these analyses and the results can be found in the Supplementary Material B.

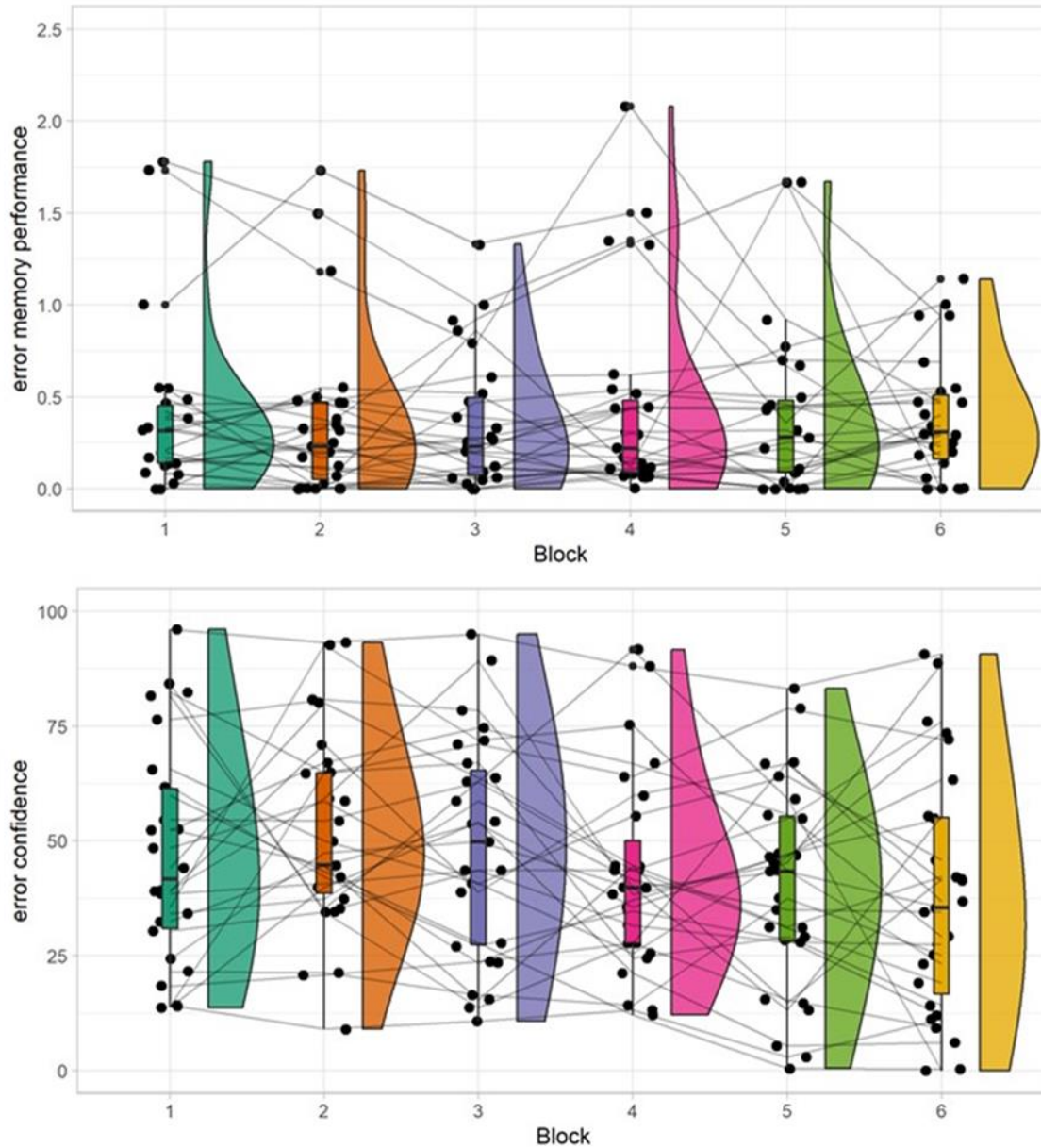


Figure 4. Top panel: Raincloud plots of participants’ error memory performance as a function of block numbers. The smaller the value, the more accuracy participants were in recalling their errors. Bottom panel: Raincloud plots of participants’ confidence rating for their error memory, as a function of block numbers. 0 means “completely not sure”, 100 means “completely sure”. For both panels, the outer shapes represent the distribution of the data over participants, the thick horizontal line inside the box indicates the group median, and the bottom and top of the box

indicate the group-level first and third quartiles of each condition. Each dot represents one participant, the thin lines in between connect the same participant's data for different blocks.

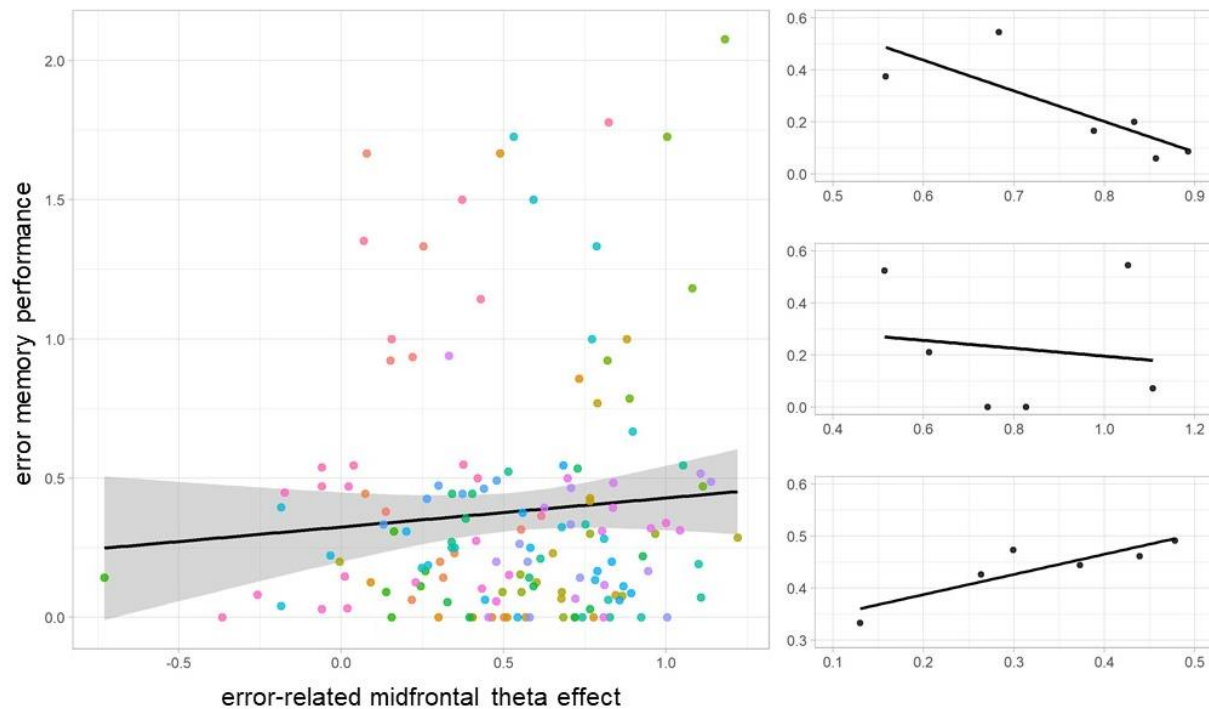


Figure 5. The relationship between the error-related midfrontal theta effect and error memory performance. Left panel: Each color codes for an individual participant and the corresponding regression line. The black regression line fits all the data points, and the gray area depicts the confidence interval. Right panel: three example participants.

Discussion

Midfrontal theta is enhanced in situations that call for more cognitive control (Cavanagh & Frank, 2014; Cavanagh et al., 2012). One of these instances is the occurrence of an error, where cognitive control is needed for subsequent behavioral adjustments (Cavanagh et al., 2012; Cohen, 2011a; Fusco et al., 2018; Luu, Tucker, & Makeig, 2004). On the other hand, midfrontal

theta also plays a crucial role in memory-related processes (Hsieh & Ranganath, 2014). For example, theta is higher during memory encoding for items that are subsequently recollected (S. Hanslmayr, Spitzer, & Bauml, 2009; Summerfield & Mangels, 2005; White et al., 2013). In the current study, we examined the link between the error-related midfrontal theta effect and participants' memory of the errors they have made.

While participants were performing a modified flanker task, we recorded their EEG activity and compared response-related theta power after erroneous and correct responses. Our results are in line with previous literature on the involvement of midfrontal theta in error processing (Cavanagh et al., 2012; Cohen, 2011a; Luu et al., 2004; Nigbur et al., 2011). Like previous studies, we observed enhanced theta power following an error commission as compared to a correct response. This error-related theta effect was present mainly in the medial frontal scalp region and in the first 500 ms after a response was made. This theta effect likely reflects error detection and the signaling of post-error cognitive control (Bonfond et al., 2017; Cavanagh & Frank, 2014; Duprez et al., 2020; Fries, 2005).

Does the detection of response errors also affect the memory of these errors? We asked participants to indicate how many errors they remembered making in each experimental block and explored the relationship between their memory performance and the trial-by-trial brain oscillation. Our results provide no evidence that error memory can be predicted by the error-related theta effect, which seems to suggest a discrepancy between the error-related and memory-related control processes. In line with the idea that the same neural implementations can be driven by distinct neuronal computation principles (Buzsaki, Anastassiou, & Koch, 2012), it is plausible that error-related and memory-related midfrontal theta have different underlying mechanisms. For instance, midfrontal theta has long been viewed as the EEG signature of the

unitary process of response conflict detection. However, it has been recently proposed that midfrontal theta reflects multiple uncorrelated processes, which give rise to comparable EEG compositions (Beldzik, Ullsperger, Domagalik, & Marek, 2022; Zuure et al., 2020). Therefore, it is plausible that even though error-related and memory-related control processes are both associated with “midfrontal theta”, the underlying neural mechanisms differ and are uncoupled. We further attempted to separate multiple theta sources and explore whether sub-component of error-related theta effect could predict error memory (Supplementary Material B). However, without high-resolution online EEG recordings, we acknowledge that the current exploration is not sufficient to fully investigate this.

An influential hypothesis is that theta oscillations may coordinate the timing of cognitive processes due to large-scale cross-frequency coupling (Duprez et al., 2020; Lisman & Jensen, 2013). Processes specific to post-error control may be linked to a specific midfrontal theta phase, while another cognitive process, like memory encoding could have a different preferential theta phase. Information arriving at specific phases would initiate multiple parallel processes in various brain regions. For instance, after error detection, communication in an extended neural network comprising of the PFC, medial temporal lobe and posterior parietal cortex might be required for subsequent memory and decision-making processes (Cohen, 2011a; Thakral, Wang, & Rugg, 2017). In concordance, it has been proposed that theta oscillations mediate top-down control from the PFC to the hippocampus for selective encoding and retrieval of episodic memories (Nyhus & Curran, 2010a). It is therefore a possibility that the initial increase in theta power after an error is made, is not predictive of subsequent error memory due to additional processing that occurs afterwards.

It could be a concern that participants during the task counted the number of errors and the error memory we tried to predict merely reflects their working memory. We consider this to be very unlikely given that (1) we asked the participants not only to report the number of errors made, but also the number of times they were too slow. Performing well on the flanker task and actively counting both the number of errors made and the times the response was too slow would be very demanding on the attentional resources and unlikely to be achieved. This is also what participants indicated when asked about strategy use at the end of the experimental session. Only two participants indicated to have used counting as a strategy, when we removed these two participants and performed the same analyses, all conclusions remain the same (Supplementary Material D). (2) The participants showed a wide range of confidence ratings, suggesting they were uncertain about the guesses rather than counting. This is again supported by the fact that participants error memory performance cannot be predicted by their working memory capacity.

Several limitations of the study should be mentioned. First, contrary to most memory studies, our measure of error-related theta does not reflect a contrast between successful and unsuccessful encoding. It would be ideal if we could dissociate errors that have been successfully and unsuccessfully encoded during the task, which however was not possible in the current design. With state-of-art pattern analysis and decoding techniques of the neural data, future studies might be able to examine this further. Second, we quantified memory accuracy as the absolute difference between recalled errors and truly committed errors. This quantification does not differentiate between errors that were forgotten (misses) and correct trials misremembered as errors (false alarms). It could be that we found no evidence for a link between error-related theta and error memory due to the pooling of these errors. Since we could not directly differentiate between misses and false alarms, we used the error under- or overestimation as a proxy and

explored its link with error-related theta. Nevertheless, our exploratory analysis (Supplementary Material C) shows no evidence that midfrontal theta can predict misses and false alarms.

To summarize, we have replicated the error-related midfrontal theta using a modified flanker task. However, the error-related theta power increase cannot predict subsequent memory performance of committed errors. These findings add to a growing literature on the PFC function in cognitive control and memory process. Still, much remains to be explored on whether midfrontal theta, a seemingly distinctive neural signature of cognitive control, reflects multiple cognitive processes.

Data Availability

Data is available at the Donders Repository (<https://data.donders.ru.nl/>). They will be shared publicly upon manuscript acceptance.

Acknowledgements

The authors would like to thank Dennis Schutter for helpful discussions, and Lara Burmeister, Lada Zelinski, and Puck Lange for their help with data collection.

Reference

- Bates, D., Maechler, M., Bolker, B., Walker, S., Christensen, R. H. B., Singmann, H., . . . Grothendieck, G. (2011). Package 'lme4'. *Linear mixed-effects models using S4 classes. R package version, 1*(6).
- Beldzik, E., Ullsperger, M., Domagalik, A., & Marek, T. (2022). Conflict-and error-related theta activities are coupled to BOLD signals in different brain regions. *Neuroimage*, 119264.
- Bonnefond, M., Kastner, S., & Jensen, O. (2017). Communication between brain areas based on nested oscillations. *eneuro*, 4(2).
- Botvinick, M. M., Cohen, J. D., & Carter, C. S. (2004). Conflict monitoring and anterior cingulate cortex: an update. *Trends in cognitive sciences*, 8(12), 539-546.
- Buzsaki, G., Anastassiou, C. A., & Koch, C. (2012). The origin of extracellular fields and currents--EEG, ECoG, LFP and spikes. *Nat Rev Neurosci*, 13(6), 407-420. doi:10.1038/nrn3241
- Cavanagh, J. F., Cohen, M. X., & Allen, J. J. (2009). Prelude to and resolution of an error: EEG phase synchrony reveals cognitive control dynamics during action monitoring. *J Neurosci*, 29(1), 98-105. doi:10.1523/JNEUROSCI.4137-08.2009
- Cavanagh, J. F., & Frank, M. J. (2014). Frontal theta as a mechanism for cognitive control. *Trends Cogn Sci*, 18(8), 414-421. doi:10.1016/j.tics.2014.04.012
- Cavanagh, J. F., Zambrano-Vazquez, L., & Allen, J. J. (2012). Theta lingua franca: a common mid-frontal substrate for action monitoring processes. *Psychophysiology*, 49(2), 220-238. doi:10.1111/j.1469-8986.2011.01293.x
- Chevalier, N., Hadley, L. V., & Balthrop, K. (2021). Midfrontal theta oscillations and conflict monitoring in children and adults. *Dev Psychobiol*, 63(8), e22216. doi:10.1002/dev.22216
- Cohen, M. X. (2011a). Error-related medial frontal theta activity predicts cingulate-related structural connectivity. *Neuroimage*, 55(3), 1373-1383. doi:10.1016/j.neuroimage.2010.12.072

- Cohen, M. X. (2011b). Hippocampal-prefrontal connectivity predicts midfrontal oscillations and long-term memory performance. *Curr Biol*, *21*(22), 1900-1905. doi:10.1016/j.cub.2011.09.036
- Cohen, M. X. (2022). A tutorial on generalized eigendecomposition for denoising, contrast enhancement, and dimension reduction in multichannel electrophysiology. *Neuroimage*, *247*, 118809. doi:10.1016/j.neuroimage.2021.118809
- Cohen, M. X., & Donner, T. H. (2013). Midfrontal conflict-related theta-band power reflects neural oscillations that predict behavior. *J Neurophysiol*, *110*(12), 2752-2763. doi:10.1152/jn.00479.2013
- Duprez, J., Gulbinaite, R., & Cohen, M. X. (2020). Midfrontal theta phase coordinates behaviorally relevant brain computations during cognitive control. *Neuroimage*, *207*, 116340.
- Eriksen, B. A., & Eriksen, C. W. (1974). Effects of Noise Letters Upon Identification of a Target Letter in a Nonsearch Task. *Perception & Psychophysics*, *16*(1), 143-149. doi:Doi 10.3758/Bf03203267
- Fries, P. (2005). A mechanism for cognitive dynamics: neuronal communication through neuronal coherence. *Trends in cognitive sciences*, *9*(10), 474-480.
- Fusco, G., Scandola, M., Feurra, M., Pavone, E. F., Rossi, S., & Aglioti, S. M. (2018). Midfrontal theta transcranial alternating current stimulation modulates behavioural adjustment after error execution. *Eur J Neurosci*, *48*(10), 3159-3170. doi:10.1111/ejn.14174
- Hanslmayr, S., Spitzer, B., & Bäuml, K.-H. (2009). Brain oscillations dissociate between semantic and nonsemantic encoding of episodic memories. *Cerebral cortex*, *19*(7), 1631-1640.
- Hanslmayr, S., Spitzer, B., & Bauml, K. H. (2009). Brain Oscillations Dissociate between Semantic and Nonsemantic Encoding of Episodic Memories. *Cerebral Cortex*, *19*(7), 1631-1640. doi:10.1093/cercor/bhn197
- Hsieh, L. T., & Ranganath, C. (2014). Frontal midline theta oscillations during working memory maintenance and episodic encoding and retrieval. *Neuroimage*, *85 Pt 2*, 721-729. doi:10.1016/j.neuroimage.2013.08.003

- Jensen, O., Gips, B., Bergmann, T. O., & Bonnefond, M. (2014). Temporal coding organized by coupled alpha and gamma oscillations prioritize visual processing. *Trends in neurosciences*, 37(7), 357-369.
- Kalfaoğlu, Ç., Stafford, T., & Milne, E. (2018). Frontal theta band oscillations predict error correction and posterror slowing in typing. *Journal of Experimental Psychology: Human Perception and Performance*, 44(1), 69.
- Kerns, J. G. (2006). Anterior cingulate and prefrontal cortex activity in an fMRI study of trial-to-trial adjustments on the Simon task. *Neuroimage*, 33(1), 399-405.
- Kreutzer, J. S., DeLuca, J., & Caplan, B. (2011). *Encyclopedia of clinical neuropsychology*: Springer.
- Lisman, J. E., & Jensen, O. (2013). The theta-gamma neural code. *Neuron*, 77(6), 1002-1016.
- Luu, P., Tucker, D. M., & Makeig, S. (2004). Frontal midline theta and the error-related negativity: neurophysiological mechanisms of action regulation. *Clin Neurophysiol*, 115(8), 1821-1835. doi:10.1016/j.clinph.2004.03.031
- Maris, E. (2012). Statistical testing in electrophysiological studies. *Psychophysiology*, 49(4), 549-565. doi:10.1111/j.1469-8986.2011.01320.x
- Maris, E., & Oostenveld, R. (2007). Nonparametric statistical testing of EEG- and MEG-data. *J Neurosci Methods*, 164(1), 177-190. doi:10.1016/j.jneumeth.2007.03.024
- Nigbur, R., Ivanova, G., & Sturmer, B. (2011). Theta power as a marker for cognitive interference. *Clinical Neurophysiology*, 122(11), 2185-2194. doi:10.1016/j.clinph.2011.03.030
- Novikov, N. A., Bryzgalov, D. V., & Chernyshev, B. V. (2015). Theta and alpha band modulations reflect error-related adjustments in the auditory condensation task. *Frontiers in Human Neuroscience*, 9, 673.
- Nyhus, E., & Badre, D. (2015). Functional organization of frontal cortex *The Wiley handbook on the cognitive neuroscience of memory* (pp. 131): Wiley.

- Nyhus, E., & Curran, T. (2010a). Functional role of gamma and theta oscillations in episodic memory. *Neurosci Biobehav Rev*, *34*(7), 1023-1035. doi:10.1016/j.neubiorev.2009.12.014
- Nyhus, E., & Curran, T. (2010b). Functional role of gamma and theta oscillations in episodic memory. *Neuroscience & Biobehavioral Reviews*, *34*(7), 1023-1035. doi:10.1016/j.neubiorev.2009.12.014
- Oostenveld, R., Fries, P., Maris, E., & Schoffelen, J. M. (2011). FieldTrip: Open Source Software for Advanced Analysis of MEG, EEG, and Invasive Electrophysiological Data. *Computational Intelligence and Neuroscience*, *2011*. doi:Artn 156869
10.1155/2011/156869
- Osipova, D., Takashima, A., Oostenveld, R., Fernández, G., Maris, E., & Jensen, O. (2006). Theta and gamma oscillations predict encoding and retrieval of declarative memory. *Journal of neuroscience*, *26*(28), 7523-7531.
- Peirce, J., Gray, J. R., Simpson, S., MacAskill, M., Hochenberger, R., Sogo, H., . . . Lindelov, J. K. (2019). PsychoPy2: Experiments in behavior made easy. *Behavior Research Methods*, *51*(1), 195-203. doi:10.3758/s13428-018-01193-y
- R Core Team. (2013). R: A language and environment for statistical computing.
- Sederberg, P. B., Kahana, M. J., Howard, M. W., Donner, E. J., & Madsen, J. R. (2003). Theta and gamma oscillations during encoding predict subsequent recall. *J Neurosci*, *23*(34), 10809-10814.
- Sederberg, P. B., Schulze-Bonhage, A., Madsen, J. R., Bromfield, E. B., McCarthy, D. C., Brandt, A., . . . Kahana, M. J. (2007). Hippocampal and neocortical gamma oscillations predict memory formation in humans. *Cereb Cortex*, *17*(5), 1190-1196. doi:10.1093/cercor/bhl030
- Summerfield, C., & Mangels, J. A. (2005). Coherent theta-band EEG activity predicts item-context binding during encoding. *Neuroimage*, *24*(3), 692-703. doi:10.1016/j.neuroimage.2004.09.012
- Thakral, P. P., Wang, T. H., & Rugg, M. D. (2017). Decoding the content of recollection within the core recollection network and beyond. *Cortex*, *91*, 101-113.

- Trujillo, L. T., & Allen, J. J. (2007). Theta EEG dynamics of the error-related negativity. *Clinical Neurophysiology*, *118*(3), 645-668.
- White, T. P., Jansen, M., Doege, K., Mullinger, K. J., Park, S. B., Liddle, E. B., . . . Liddle, P. F. (2013). Theta power during encoding predicts subsequent-memory performance and default mode network deactivation. *Hum Brain Mapp*, *34*(11), 2929-2943. doi:10.1002/hbm.22114
- Wynn, S. C., Daselaar, S. M., Kessels, R. P. C., & Schutter, D. J. L. G. (2019). The electrophysiology of subjectively perceived memory confidence in relation to recollection and familiarity. *Brain Cogn*, *130*, 20-27. doi:10.1016/j.bandc.2018.07.003
- Yordanova, J., Falkenstein, M., Hohnsbein, J., & Kolev, V. (2004). Parallel systems of error processing in the brain. *Neuroimage*, *22*(2), 590-602.
- Zuure, M. B., Hinkley, L. B., Tiesinga, P. H., Nagarajan, S. S., & Cohen, M. X. (2020). Multiple midfrontal thetas revealed by source separation of simultaneous MEG and EEG. *Journal of neuroscience*, *40*(40), 7702-7713.

Supplementary Materials

Supplementary Material A: (generalized) linear mixed effect models

for accuracy

```
glmer(accuracy ~ congruency + post_error + WM_sum + ordered(block) + (1 + congruency +  
post_error | participant), data = data_by_trial, family = "binomial", control =  
glmerControl(optimizer = "bobyqa"))
```

for RT

```
lmer(log(RT) ~ congruency + accuracy + post_error + WM_sum + ordered(Block) + (1 +  
congruency + accuracy + post_error | participant), data = data_by_trial, control =  
lmerControl(optimizer = "bobyqa"))
```

for error memory performance

```
glmmTMB(error_memory_abs ~ theta_effect + error_rate + WM_sum + ordered(block) + (1 +  
error_rate | participant), data= data_by_block., family = ziGamma(link = "log"), ziformula=~1)
```

additional analysis

for error memory performance (over- vs. under-estimation)

```
glmer(error_memory_sign ~ theta_effect + error_rate + ordered(block) + (1 | participant), data =  
data_by_block, family = "binomial", control = glmerControl(optimizer = "bobyqa"))
```

for error memory performance: incl. confidence

```
glmmTMB(error_memory_abs ~ theta_effect * confidence + error_rate + WM_sum +  
ordered(block) + (1 + error_rate | participant), data = data_by_block, family = ziGamma(link =  
"log"), ziformula=~1)
```

*## for error memory performance: theta effects computed using midfrontal theta components and
other components from generalized eigendecomposition*

```
glmmTMB(error_memory_abs ~ theta_effect_ged_mft + error_rate + WM_sum +  
ordered(block) + (1 + error_rate | participant), data = data_by_block, family = ziGamma(link =  
"log"), ziformula=~1)
```

```
glmmTMB(error_memory_abs ~ theta_effect_ged_other + error_rate + WM_sum +  
ordered(block) + (1 + error_rate | participant), data = data_by_block, family = ziGamma(link =  
"log"), ziformula=~1)
```

*## for error memory performance: theta effects computed using phase-locked vs. non-phase-
locked theta*

```
glmmTMB(error_memory_abs ~ theta_effect_phase_locked + error_rate + WM_sum +  
ordered(block) + (1 + error_rate | participant), data = data_by_block, family = ziGamma(link =  
"log"), ziformula=~1)
```

```
glmmTMB(error_memory_abs ~ theta_effect_non_phase_locked + error_rate + WM_sum +  
ordered(block) + (1 + error_rate | participant), data = data_by_block, family = ziGamma(link =  
"log"), ziformula=~1)
```

*all continuous predictors in the models are centered.

Supplementary Material B: additional analysis on whether sub-components of midfrontal theta predicts error memory

Phase-locked and non-phase-locked power

For the calculation of the non-phase-locked power, we computed the event-related-potentials per condition (correct vs. incorrect) per block and subtracted these from the time-domain EEG signal. This was done per trial, per electrode, and per participant. The (time-)frequency information was then extracted using the same method we extract the total power (i.e., methods described in the methods section of the manuscript). The phase-locked power was computed by subtracting the non-phase-locked power from the total power (Cohen & Donner, 2013). The generalized linear mixed effect model showed that neither phase-locked theta power ($\beta = 0.008$, $SE = 0.01$, $z = 0.68$, $p = .50$) nor non-phase-locked theta power ($\beta = -0.11$, $SE = 0.21$, $z = -0.51$, $p = .61$) predicts error memory.

Midfrontal theta versus other theta sources

We used a feature-driven multivariate source separation method that was optimized to determine whether theta activity reflects a linear summation of independent sources, called generalized eigendecomposition (GED). We followed the steps outlined in Cohen (2021) to compute the GED component time series. As in Zuure (2020), the signal matrix was bandpass-filtered data at theta frequency (4-7 Hz) and the reference matrix the broadband (0.1 - 30 Hz) data. Our GED analysis thus involved a spectral contrast tailored to maximize the signal-to-reference ratio between theta and broadband signal. Once the GED components were obtained, a permutation analysis was performed to select only the significant components ($\alpha = .05$). Out of those, the main midfrontal theta components were chosen based on visual inspection of the component

maps, one component per participant. The remaining significant components were averaged together to represent the additional theta power, labeled “other”. Generalized linear mixed effect model showed that neither the main midfrontal theta component ($\beta = 0.04$, $SE = 0.20$, $z = 0.21$, $p = .83$) nor the average of the “other” theta components ($\beta = 0.20$, $SE = 0.20$, $z = 0.98$, $p = .33$) predicts error memory.

Supplementary Material C: additional analysis on whether midfrontal theta predicts the sign of error memory

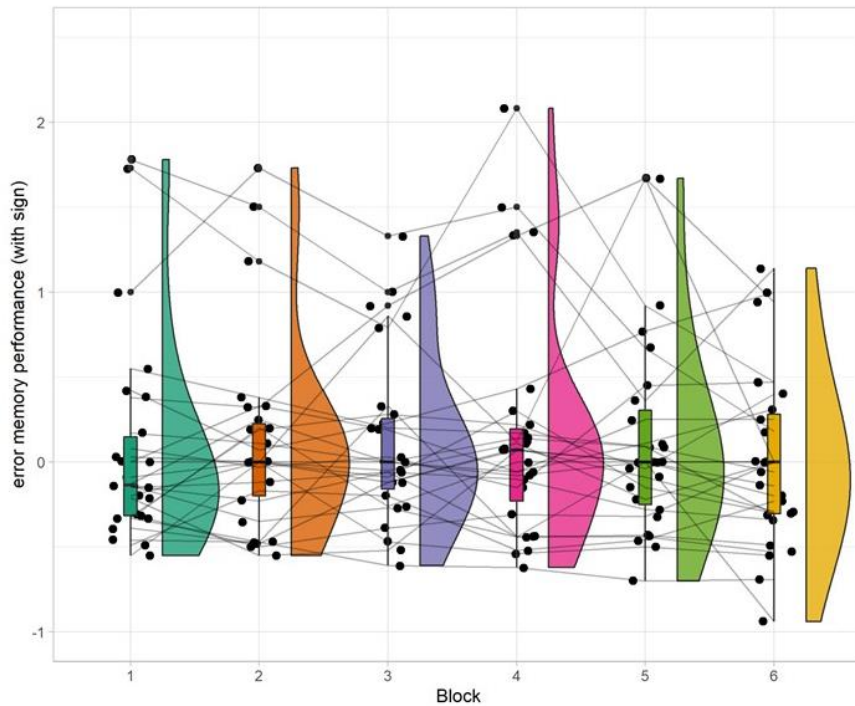


Figure S1. Raincloud plots of participants' estimation memory performance, computed as:

$$\frac{Error_{recall} - Error_{true}}{Error_{true}}$$

A positive value means overestimating, a negative value means underestimating. The outer shapes represent the distribution of the data over participants, the thick horizontal line inside the box indicates the group median, and the bottom and top of the box indicate the group-level first and third quartiles of each condition. Each dot represents one participant, the thin lines in between connect the same participant's data for different blocks.

In general, participants tend to overestimate rather than underestimate the number of errors they made (Figure S1). However, this cannot be predicted by their error-related midfrontal theta effect

($\beta = -1.07$, $SE = 0.92$, $z = -1.16$, $p = .25$). Additionally, although participants tend to underestimate when they make more errors ($\beta = -15.73$, $SE = 4.71$, $z = -3.34$, $p < .001$), their tendency to over- or underestimate do not change over time ($\beta = 0.23$, $SE = 0.57$, $z = 0.41$, $p = .68$).

Supplementary Material D: additional analysis excluding two subjects who used the counting strategy

To make sure that our results are not confounded by participants who possibly used a counting strategy, we asked all the participants at the end of the Flanker task to report if they have been using counting as a strategy. Subsequently we excluded two of the participants who reported to do so and performed the main analysis again. The results were comparable to the ones reported in the paper.

The cluster-based permutation analysis on the TFRs (Figure S2) again revealed a significant positive cluster ($p < .001$) with the same temporal characteristics. Specifically, this cluster was most pronounced between -31 ms and 506 ms relative to response onset.

In Figures S3 we show participant' ability to remember their errors across blocks, and their confidence of their error memory, respectively. Again, Figure S4 shows that there is no clear relationship between the error-related theta effect and the memory performance, supported by the generalized linear mixed effects model ($\beta = -0.05$, $SE = 0.24$, $z = -0.22$, $p = .82$).

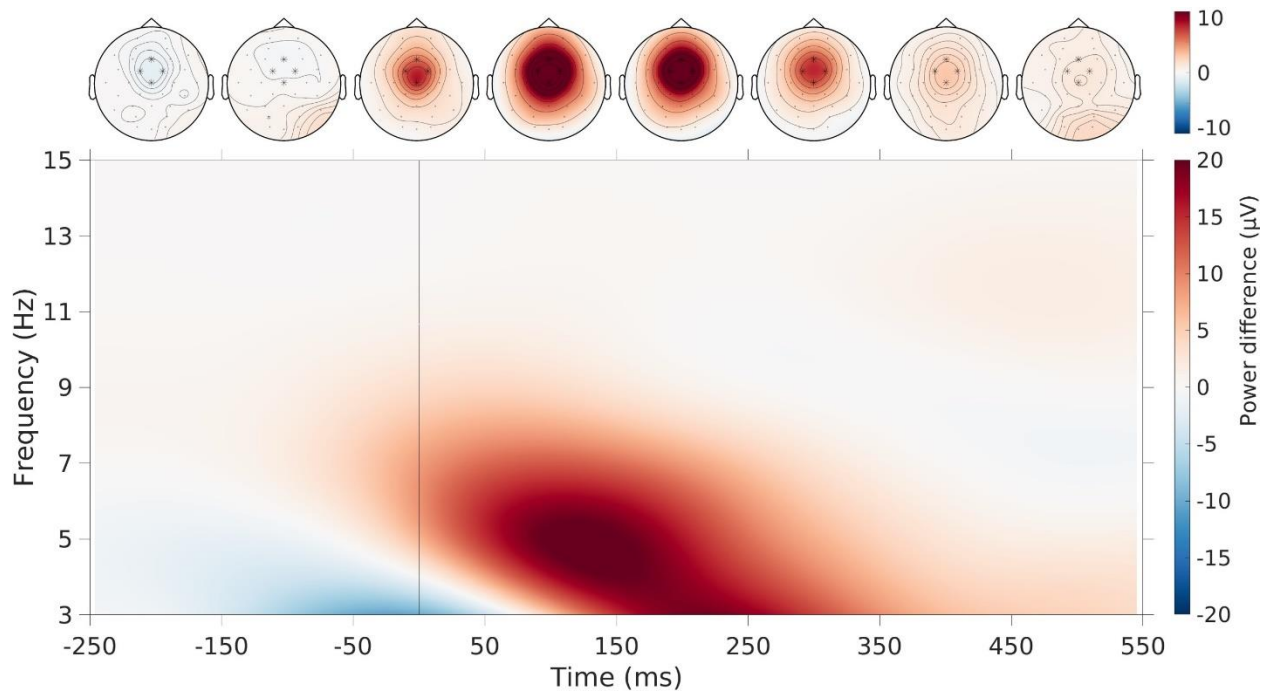


Figure S2. The theta power difference between error and correct trials over time. All time windows are relative to response onset. On the top row the topographical distribution of the effect is plotted, with the midfrontal channels marked (FC1, FC2, Fz, Cz). The time-frequency representation for these midfrontal channels is plotted on the bottom row (excluding two additional participants who used counting strategy).

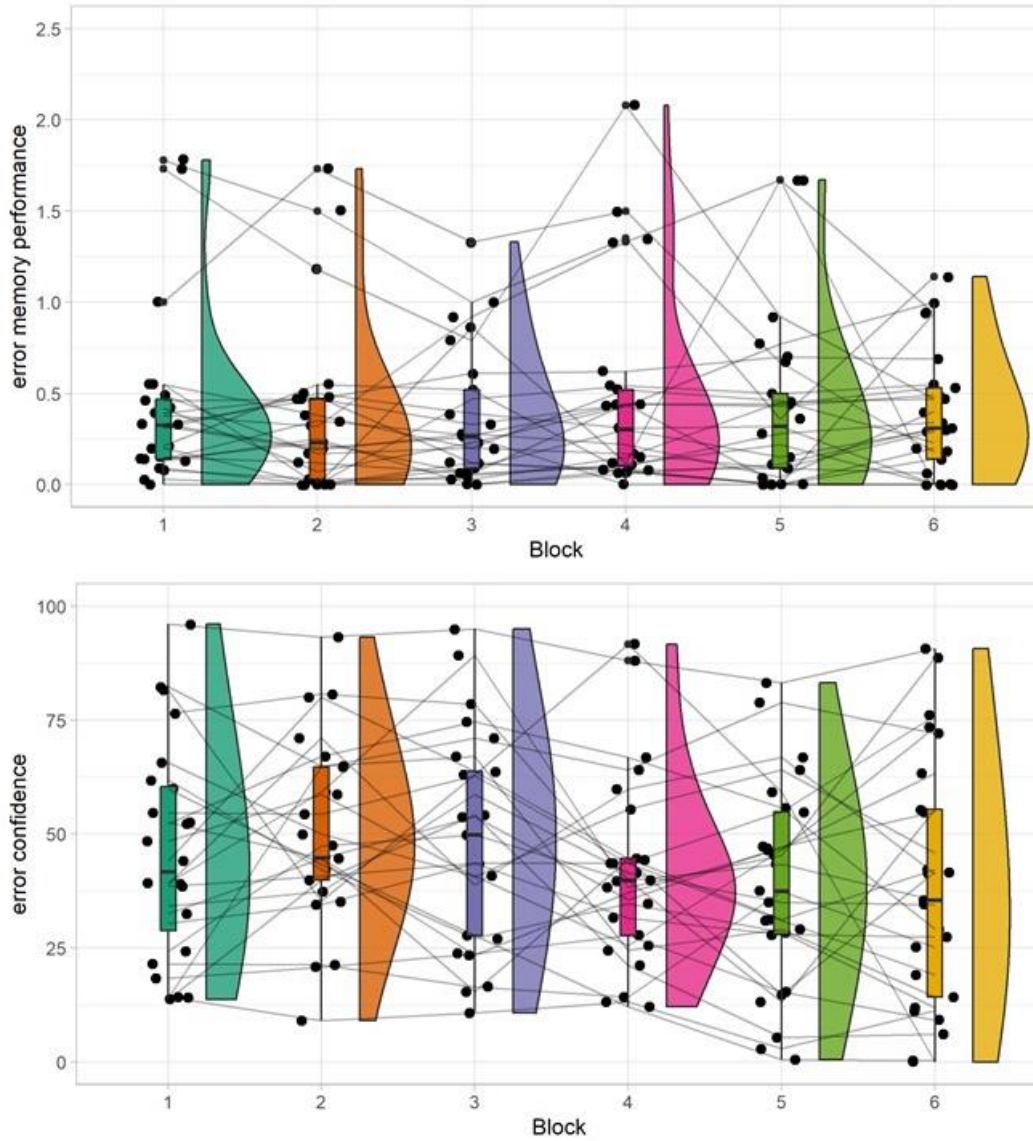


Figure S3. Raincloud plots of participants' error memory performance (top panel) and confidence rating for their error memory (bottom panel) as a function of block numbers (excluding two additional participants who used counting strategy).

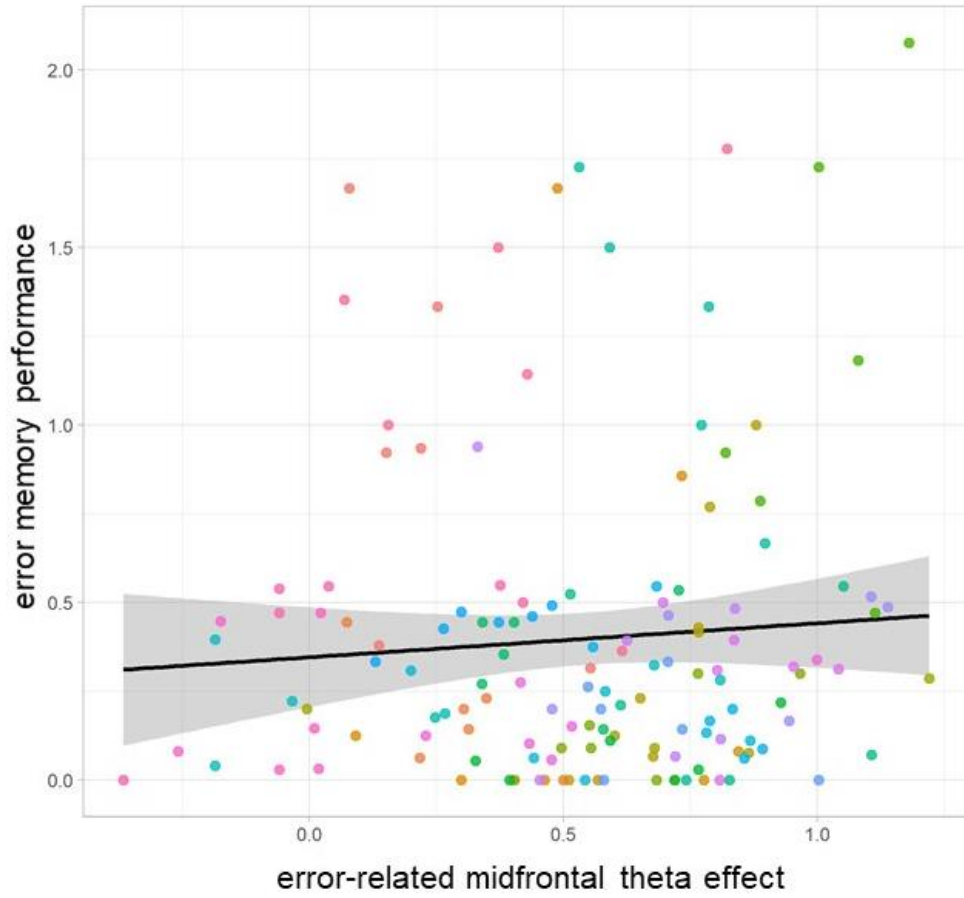


Figure S4. The relationship between the error-related midfrontal theta effect and error memory performance (excluding two additional participants who used counting strategy).